Mercury emission profile for the torrefaction of sewage sludge at a full-scale plant and application of polymer sorbent

AUTHOR(S):

Cheng, Yingchao; Asaoka, Yuki; Hachiya, Yoshiyuki; Moriuchi, Naoki; Shiota, Kenji; Oshita, Kazuyuki; Takaoka, Masaki

CITATION:

Cheng, Yingchao ...[et al]. Mercury emission profile for the torrefaction of sewage sludge at a full-scale plant and application of polymer sorbent. Journal of Hazardous Materials 2022, 423(Part B): 127186.

ISSUE DATE:

2022-02-05

URL:

http://hdl.handle.net/2433/282757

Journal of Hazardous Materials 423 (2022) 127186

Contents lists available at ScienceDirect

Journal of Hazardous Materials

journal homepage: www.elsevier.com/locate/jhazmat

Mercury emission profile for the torrefaction of sewage sludge at a full-scale plant and application of polymer sorbent

Yingchao Cheng [a,b], Yuki Asaoka [c], Yoshiyuki Hachiya [c], Naoki Moriuchi [d], Kenji Shiota [a], Kazuyuki Oshita [a], Masaki Takaoka [a,*]

[a] Department of Environmental Engineering, Ce School of Engineering, Kyoto University, Katsura, Nisikyo-ku, Kyoto 615-8540, Japan
[b] Global Resource Sustainability Research Section, Material Cycles Division, National Institute for Environmental Studies, 16-2 Onogawa, Tsukuba 305-8506, Japan
[c] Tsukishima Kikai Co., Ltd. Solution, Technology Department, 3-5-1, Harumi, Chuo-ku, Tokyo 104-0053, Japan
[d] W. L. Gore & Associates, G.K.-14 F, W Building, 1-8-15 Konan, Minato-ku, Tokyo 108-0075, Japan

ARTICLE INFO

Editor: Dr. L. Angela Yu-Chen

Keywords:
Mercury adsorption
Sorbent polymer catalyst composite material
GORE Mercury Control System
Thermodynamic calculation
Speciation mercury continuous emission monitoring

ABSTRACT

We evaluated mercury (Hg) behavior in a full-scale sewage sludge torrefaction plant with a capacity of 150 wet tons/day, which operates under a nitrogen atmosphere at a temperature range of 250–350 °C. Thermodynamic calculations and monitoring results show that elemental Hg (Hg^0) was the dominant species in both the pyrolysis gas during the torrefaction stage and in the flue gas from downstream air pollution control devices. A wet scrubber (WS) effectively removed oxidized Hg from the flue gas and moved Hg to wastewater, and an electrostatic precipitator (ESP) removed significant particulate-bound Hg but showed a limited capacity for overall Hg removal. Hg bound to total suspended solids had a much higher concentration than that of dissolved Hg in wastewater. Total suspended solid removal from wastewater is therefore recommended to reduce Hg discharge. Existing air pollution control devices, which consist of a cyclone, WS, and ESP, are not sufficient for Hg removal due to the poor Hg^0 removal performance of the WS and ESP; a further Hg^0 removal unit is necessary. A commercial packed tower with sorbent polymer catalyst composite material was effective in removing Hg (83.3%) during sludge torrefaction.

1. Introduction

Sewage sludge is a biomass product generated in the wastewater treatment process. Sludge accumulates nutrients (Mayer et al., 2016; Zhao et al., 2018), heavy metals (Mulchandani and Westerhoff, 2016; Santos and Judd, 2010; Westerhoff et al., 2015), and energy potential (Peccia and Westerhoff, 2015). Typical methods for sludge treatment include anaerobic digestion (Cao and Pawłowski, 2012; Song et al., 2004; Stasinakis, 2012) and thermal processes (Zhang et al., 2017) such as incineration (Cheng et al., 2020), torrefaction (Atienza-Martínez et al., 2015, 2013), carbonization (Tasca et al., 2019; Van Wesenbeeck et al., 2014; Xu et al., 2020; Zheng et al., 2019), and pyrolysis (Li and Feng, 2018; Raheem et al., 2018). Thermal treatment, especially incineration, is widely used in Japan due to its advantage of volume reduction (Takaoka et al., 2012).

Sludge torrefaction, an emerging thermal treatment method, is often described as a mild form of pyrolysis (Tumuluru et al., 2011). In this process, sludge is heated in an inert (such as nitrogen) and reduced atmosphere at temperatures of 200–300 °C, lower than the temperature of conventional carbonization (Basu, 2013; Prins et al., 2006). Torrefaction can convert sludge into a carbon-containing product useable as biofuel (Park and Jang, 2011a, 2011b), which is considered a storable energy carrier (Axelsson et al., 2012; Titirici et al., 2007; Zhang et al., 2017). With the characteristics of brown coal, the biofuel can be co-fired with fossil coal to generate electricity in power plants (Park and Jang, 2011a, 2011b). Moreover, as the 2 °C warming target and low carbon footprint require the utilization of biofuels, torrefaction may gain further popularity as a sludge treatment. In Japan, fuel production from sludge has been increasing, with 8% of the total sludge converted into fuel in Japan at 20 plants (including 7 low-temperature torrefaction plants) in

Abbreviations: APCDs, air pollution control devices; WSD, wet scrubber for drying; ESP, electrostatic precipitator; GMCS, GORE Mercury Control System; Hg^0, elemental mercury; Hg^{2+}, oxidized mercury; Hg^p, particulate-bounded mercury; Hg-CEM, speciation mercury continuous emission monitors; SPC, sorbents polymer catalyst; THg, total mercury; TP, torrefaction plant; *TSS*, total suspended solids; WS, wet scrubber.

* Corresponding author.
E-mail address: takaoka.masaki.4w@kyoto-u.ac.jp (M. Takaoka).

https://doi.org/10.1016/j.jhazmat.2021.127186
Received 13 June 2021; Received in revised form 19 August 2021; Accepted 7 September 2021
Available online 11 September 2021

operation in 2019 MLIT (Ministry of Land, Infrastructure, Transport and Tourism).

During sludge torrefaction, heavy metals in the sludge may be distributed among the biofuel, flue gas, and wastewater generated at the air pollution control devices (APCDs). Tomasi Morgano et al. (2018) reported that metals and other minerals were completely retained in the char from sludge pyrolysis at 350–500 °C, with the exception of mercury (Hg). As a toxic pollutant, Hg is harmful to humans after intake via fish consumption or inhalation (Holmes et al., 2009; Zhang and Wong, 2007). In 2017, the Minamata Convention on Hg came into force, which is expected to lead to reductions in the emission and release of Hg. Coal-fired power plants are considered the most significant anthropogenic sources of Hg emissions in most countries (Friedli et al., 2004; Pacyna et al., 2010; Srivastava et al., 2006; Yang et al., 2007). Municipal solid waste and sludge incineration are also essential sources of anthropogenic Hg emissions (Takaoka et al., 2012, 2002), and Hg released from municipal sewage may be a major source of the total anthropogenic Hg released into aquatic environments in China (Liu et al., 2018). As is the case with incineration, the increase of sludge torrefaction use in Japan may be an emerging source for Hg emissions into the atmosphere. In Japan, total Hg (THg) emission from the stacks of existing and newly constructed waste and sludge thermal treatment plants has been limited to 50 and 30 μg/Nm^3, respectively, since 1 April 2018 (Takiguchi and Tamura, 2018).

To date, Hg behavior in sludge torrefaction has been poorly investigated, and existing research is limited to lab-scale tests (Atienza-Martínez et al., 2015, 2013). While the speciation of Hg, which includes oxidized Hg (Hg^{2+}), particulate-bound Hg (Hg^p), and elemental Hg (Hg^0) (Galbreath and Zygarlicke, 2000), affects the removal of Hg by APCDs, almost no research has investigated the species of Hg associated with sludge torrefaction. Although temperature has a significant influence on the speciation of Hg in flue gas (Reed et al., 2001), there are few reports on the evolution of the dominant Hg species removed by APCDs due to the temperature change in sludge torrefaction. Moreover, the evolutionary mechanism of the dominant Hg species, which can be explained by thermodynamic calculations, has not been fully described.

Therefore, the purposes of this study are to provide a comprehensive investigation of Hg behavior in a full-scale sludge torrefaction plant, including the concentration of Hg and evolution of Hg species in sludge, biofuel, flue gas, and wastewater, and to compile a complete mass balance throughout the torrefaction process. We conducted thermodynamic calculations to elucidate the dominant Hg species present during sludge torrefaction. In addition, we tested and evaluated the adsorptive removal performance of Hg^0 using a commercial sorbent polymer catalyst (SPC) composite material in the torrefaction plant, which has also been tested for Hg removal in Poland and Germany and used in the US due to its advantages of high capacity and operation in wet gas streams (Ebert, 2013; Sloss, 2017).

2. Materials and methods

2.1. Torrefaction plant

A full-scale torrefaction plant (**TP**) in eastern Japan was selected for this study. It has a capacity of 150 wet tons/day (water content, 80.4%) for sludge treatment. Prior to torrefaction, the sludge was pre-dried at 100 °C, producing steam by heating of treated wastewater with waste heat from the secondary combustion furnace, and then granulated. The flue gas generated at the sludge dryer was treated at the wet scrubber for drying (WSD) and combusted at the secondary combustion furnace. Then, the pre-dried granular sludge was baked under a nitrogen atmosphere to a temperature range of 250–350 °C to produce biofuel in the torrefaction furnace. During torrefaction, pyrolysis gas was generated. The pyrolysis gas is a mixture of H_2O (60%), C_5H_{12} (20%), CO_2 (12%), N_2 (5%), CO (2%), and other components. The pyrolysis gas was combusted in a secondary combustion furnace connected to the **TP** at 900–960 °C. Thereafter, flue gas generated from the secondary combustion furnace was treated with APCDs, which originally included a cyclone, wet scrubber (WS), and wet electrostatic precipitator (ESP) (Fig. 1).

2.2. Hg adsorption by a packed tower with sorbent polymer catalyst composite material

To reduce Hg emission from the stack, we used a packed tower with SPC composite material downstream of the existing APCDs at the **TP**. The SPC composite material (W. L. Gore & Associates, Inc.) was used in the tower to test the adsorptive removal of Hg at **TP**. The SPC used for Hg removal has recently been adopted in coal-fired plants and sewage sludge incinerators in the US as the GORE Mercury Control System (GMCS). This system typically comprises a tower containing several layers, and an eight-layer tower was used in this study. The GMCS treats flue gas with a Hg concentration as high as 250 μg/Nm^3 and can decrease the Hg concentration to as low as 1 μg/Nm^3 by increasing the number of layers. The fixed sorbent can capture Hg^0 and gas-phase Hg^{2+} from industrial flue gas. Schematics of the adsorption units used for the polymer tower at the **TP** are shown in Fig. 1. The adsorption test was conducted from August 15, 2017, to December 18, 2017. Data were collected on 105 days during this period. Data were not available for several days during that period due to failure of the monitoring devices.

2.3. The sampling process

Batch sampling was conducted at the **TP** to obtain solid and water samples (Fig. 1). For flue gas, the Ontario Hydro Method was used for sampling. In this method, a sample is withdrawn from the flue gas stream isokinetically through a probe and filter system, maintained at 120 °C or the flue gas temperature (whichever is greater), and then subjected to a series of impingers in an ice bath. Particle-bound Hg is collected on a quartz fiber filter. Hg^{2+} is collected in the impingers, which contain chilled 1.0 mol/L KCl solution. Hg^0 was collected in subsequent impingers (one impinger containing chilled 5% HNO_3 and 10% H_2O_2 solution and three impingers containing chilled 10% H_2SO_4 and 4% $KMnO_4$ solution) (ASTM D6784-02, 2002). In addition to manual sampling and measurement of the flue gas, continuous emission monitors for Hg speciation (Hg-CEM, Nippon Instruments Co., Ltd., Tokyo, Japan) were employed before and after the polymer tower at the **TP** to monitor Hg behavior during the adsorption test, as shown in Fig. 1.

2.4. Analytical methods

2.4.1. Analysis of solid and liquid samples

Solid and liquid samples were measured by the heat-vaporization method using the MA-2000 analyzer (Nippon Instruments Co., Ltd., Japan) soon after sampling. Hg was collected as a gold amalgam and detected using cold-vapor atomic absorption spectrometry (Löthgren et al., 2007). The detection limit of the analyzer was 0.002 ng.

2.4.2. Manual gaseous Hg measurement

For flue gas, after sampling in a solution with the impinger, the Hg concentration was measured using a reducing-vaporization Hg analyzer (RA-4300; Nippon Instruments Co. Ltd., Japan). Stannous chloride was used as a reducing agent, and bubbling with stannous chloride transformed the Hg ions into Hg vapor, which was directed onto an absorption cell. All Hg concentrations in the flue gas were corrected for 12% oxygen concentration.

2.4.3. Hg continuous emission monitor

The Hg-CEM was developed by Nippon Instruments and the Central Research Institute of the Electric Power Industry in Japan. One unit of the Hg-CEM consists of the MS-1A pre-treater and DM-6B detector (Nippon Instruments) (Takaoka et al., 2012), which can measure both

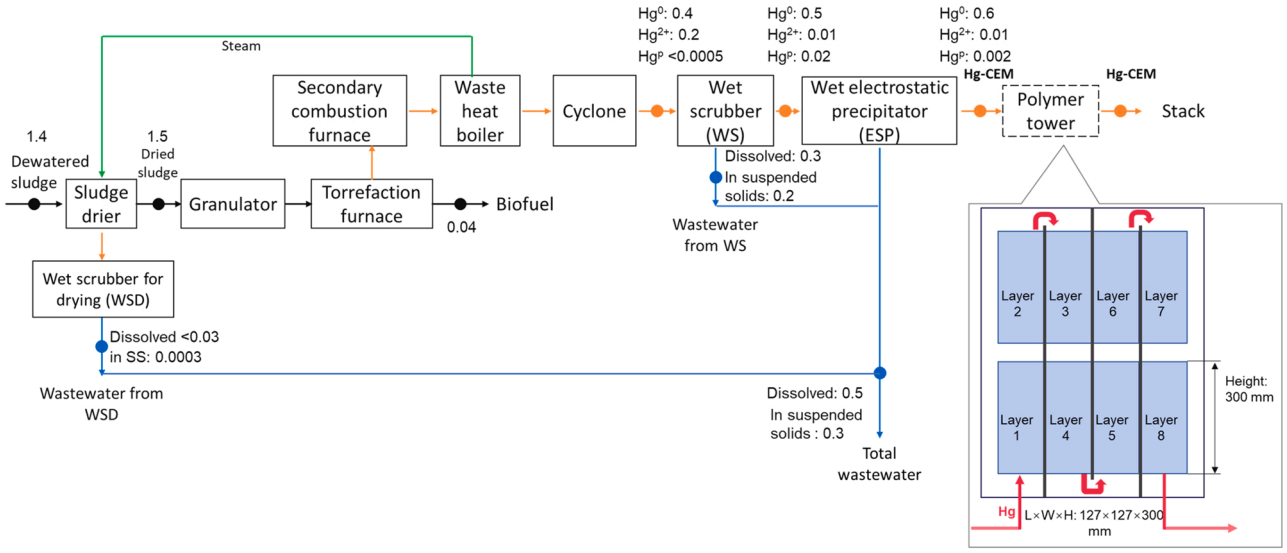

Fig. 1. Schematics of sample collection from **TP**. Solid samples, including dewatered sludge, dried sludge, and generated biofuel, were collected. For water samples, wastewater from the WSD at the drying unit and wastewater from WS at the APCDs were collected separately, while total wastewater was a mixture of all wastewaters from WSD, WS, and ESP. The green arrow shows the flow of steam. The black, blue, and orange arrows (dots) show the mass flows (sampling points) of solids, water, and flue gas, respectively. Hg-CEM: mercury continuous emission monitor. The numbers aside from the arrows show the average hourly mass flow of Hg in **TP** (Unit: g/h). The figure in the box shows the adsorption unit for the polymer tower at **TP**. Flue gas flows from the bottom to the top of the polymer tower.

Hg^0 and Hg^{2+}, was set before the polymer tower. The other unit of the Hg-CEM consists of WLE and EMP-2, also developed by Nippon Instruments. The detection limit of this device is 0.1 μg/Nm^3 (Takaoka et al., 2018). This set can only measure the THg in the flue gas and was set after the polymer tower.

2.5. Thermodynamic calculation

We calculated thermodynamic equilibrium in the **TP** using *FactSage* software (version 6.1) to simulate the species of Hg (Cheng et al., 2020). The species composition of Hg was calculated over temperature ranges of 240–420 °C and 100–1000 °C for the torrefaction furnace and secondary combustion furnace, respectively. Experimental data (Table 1) on the composition of the feed sludge and operating conditions were used as the input data for *FactSage* software. Although Cl is not a major element in sludge, it was used in the thermodynamic calculations due to its significant influence on the speciation of Hg (Edwards et al., 2001; Kellie et al., 2005; Lei et al., 2007; Preciado et al., 2014; Zhang et al., 2012). The input data for the torrefaction and secondary combustion furnaces at the **TP** are summarized in Tables A.1 and A.2.

2.6. Quality assurance

For the Hg-CEM, we checked the sensitivity of the monitor using a standard Hg generation device (MGS-1; Nippon Instruments Co. Ltd., Japan) both before and after the sampling campaign. During the sampling process, the sensitivity of the monitors was stable, and the Hg-CEM calibrated its baselines automatically with the zero gas (clean air without mercury) every 58 min.

For liquid samples, blank samples (ultrapure water) were prepared together with test samples to confirm the samples were not contaminated at the sampling and storage stages. The recovery rate of Hg for the measurement was also confirmed by adding a known concentration of Hg to the absorbent solution. During the measurement of both solid and liquid samples, correlation factors no less than 0.9999 were assured for the calibration curves.

3. Results and discussion

3.1. Concentrations and species evolution of Hg in sludge, biofuel, flue gas, and wastewater and the influence of temperature

To comprehensively evaluate Hg behavior during sludge

Table 1
Concentration and speciation of Hg in sludge, biofuel, water, and flue gas in **TP.**

	Solid			Treated	Wastewater			Flue gas		
	Dewatered sludge	Dried sludge	Biofuel	water	from WSD	from WS	Total	Inlet of WS	Outlet of WS	Stack
Flow rate	tons/day				m^3/day			Nm^3/h (dry)		
	152.2	37.3	20.5		1654	147	2195	5400	5300	5700
TS/*TSS*	%				mg/L					
	18.2	74.2	95.1	2.0	5.1	70	250			
c_{Hg} (overall)	mg/kg-dry solid				mg/L			μg/Nm^3		
	1.2	1.3	0.05	< 0.0005	< 0.0005	0.089	0.0091	108	93.7	98.17
c_{Hg} in *TSS*					mg/kg					
				1.8	0.95	520	15			
								μg/Nm^3		
c_{Hg0} gaseous								79	88	97
c_{Hg2+} gaseous								29	2.3	0.88
c_{Hg} particulate								< 0.1	3.4	0.29

TS: Total solids content; *TSS*: Total suspended solids; WSD: Wet scrubber for drying; WS: wet scrubber.

torrefaction, we sampled and analyzed the concentrations and speciation of Hg in each stream at **TP** including sludge, biofuel, pyrolysis gas, flue gas, and wastewater from APCDs.

3.1.1. Sludge

During the sludge drying stage (Fig. 1), the concentration of Hg in dewatered sludge was 1.2 mg/kg-dry (Table 1), consistent with the Hg concentration in sludge from the study area of 1.3 ± 0.5 mg/kg-dry. This Hg concentration is comparable with previous research conducted in Japan, which reported concentrations of 1.24–1.29 mg/kg-dry (Takaoka et al., 2012). After drying, the Hg concentration barely changed in the dried sludge, reaching 1.3 mg/kg-dry. Thus, the moisture lost in the drying process removed negligible Hg. As a result, the wastewater from the WSD has a very low Hg concentration of less than 0.0005 mg/L. This result is consistent with our previous study on sewage sludge drying in an incineration plant (Cheng et al., 2020). The Hg species present in sludge may be the reason for the stability of the Hg distribution throughout the drying process. When Hg occurs as Hg^0 in dewatered sludge, it tends to escape into the gas phase during the drying process, resulting in a decrease in the Hg concentration in the dried sludge. As the Hg concentration in the dried sludge did not decrease, the Hg species in the dewatered sludge is most likely Hg^{2+}, which is more stable at high temperatures (Cheng et al., 2019; Janowska et al., 2017).

3.1.2. Biofuel

In the torrefaction furnace, on the other hand, biofuel showed a Hg concentration of 0.05 mg/kg-dry (Table 1), which was much lower than levels in the dewatered and dried sludge. The low Hg concentration in biofuel indicates a shift in Hg between the solid and gas phases during torrefaction under a nitrogen atmosphere. Thermodynamic calculation results (Fig. 2(a)) showed that all Hg species present occur in the gas phase. The low torrefaction temperature of 250–350 °C under a nitrogen atmosphere enables Hg^0 to be the dominant Hg species (almost 100%), indicating that the torrefaction process reduced Hg^{2+} in the dried and granulated sludge into Hg^0 in the gas phase. Thus, the torrefaction furnace converted dried and granulated sludge into biofuel while transferring Hg into pyrolysis gas in the form of Hg^0.

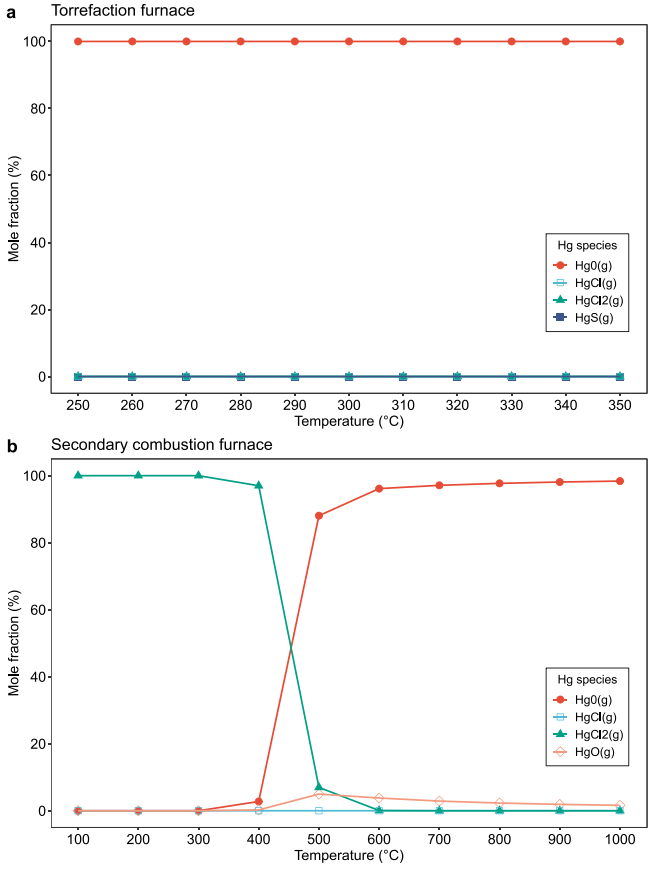

Fig. 2. Thermodynamic calculation results for the species of Hg in (a) torrefaction furnace (250–350 °C) and (b) secondary combustion furnace (100–1000 °C). All Hg species exist in the gas phase (g).

3.1.3. Pyrolysis gas and flue gas

In the pyrolysis gas from the torrefaction furnace, Hg^0 is the dominant Hg species according to our thermodynamic calculations (Fig. 2(a)) due to the inert and reduced atmosphere. The pyrolysis gas was incinerated in the secondary combustion furnace with auxiliary fuels including sludge digestion gas, natural gas, purge gas from the sludge drier, and combustion air at 900–960 °C (Table A.2). In flue gas generated in the secondary combustion furnace at temperatures higher than 500 °C, Hg^0 was the dominant Hg species (Fig. 2(b)). This finding is in accordance with our previous research on sewage sludge mono-incinerators (Cheng et al., 2020).

Waste heat in the flue gas from the secondary combustion furnace was utilized in the boiler to produce steam for the sludge drier. Then, the flue gas was treated with APCDs (Fig. 1), and its temperature decreased from ~900 °C to 64 °C during this process prior to emission from the stack. This decrease in temperature may cause a shift in the dominant Hg species from Hg^0 to Hg^{2+}, possibly in the form of $HgCl_2$, given sufficient Cl existed as the oxidant (Tables A.1 and A.3), as estimated from thermodynamic calculations (Fig. 2(b)). Thus, at the inlet of the WS (~200 °C), Hg^0 accounted for 73% (79 μg/Nm^3) of the THg concentration (108 μg/Nm^3), and Hg^{2+} increased to account for 27% (29 μg/Nm^3) (Table 1). Not all Hg^0 became Hg^{2+}, as the retention time of flue gas in the APCDs might be shorter than the chemical reaction time needed for the evolution of Hg species. The WS effectively lowered the Hg^{2+} level from 29 μg/Nm^3 at the inlet to 2.3 μg/Nm^3 at the outlet due to the high solubility of Hg^{2+} (US EPA, 2001; Chalkidis et al., 2020). At the outlet of the WS, the Hg^0 concentration increased slightly (Table 1). The increase in Hg^0 at the WS may be caused by re-emission due to the reduction of Hg^{2+} by aqueous S(IV) (sulfite and/or bisulfite) or halides ligands (Cl and ClO^-) in the WS (Cheng et al., 2013; Omine et al., 2012; Hsu et al., 2021), which also occurs in the WS of sewage sludge incinerators (Cheng et al., 2020).

With Hg^{2+} accounting for a very small fraction (0.4–6.1 μg/Nm^3, 1–3%) of the flue gas after WS, Hg^0 was dominant and fluctuated significantly from 35.4 to 198 μg/Nm^3 (Fig. 3(a)). By correlating the Hg concentration in the flue gas with the temperature of the torrefaction furnace, we found that the Hg^0 concentration in the flue gas increased at temperatures of 250–350 °C (Fig. 3(b)). Hg fractionation did not change with temperature, although the concentrations of both emitted Hg^0 and Hg^{2+} increased ($p < 0.005$). This pattern is similar to that reported previously in the woody biomass torrefaction process (Dziok, 2020), in which the amount of Hg removed from biomass increased with temperature, and the greatest increase in Hg removal was achieved in the temperature range of 250–300 °C.

At the stack, the THg concentration was almost the same as that at the outlet of the WS, and Hg^0 was the dominant species. Thus, the ESP barely oxidized or removed Hg^0, despite the low temperature (64 °C) at the ESP that enables a higher Hg removal rate. This result differs from previous findings in coal-fired power plants and municipal solid waste incinerators, in which the ESP removed 20–50% of Hg (Meij and te Winkel, 2006; Takahashi et al., 2010), and small amounts of Hg^0 were oxidized to Hg^{2+} (Wang et al., 2010). The poor Hg removal performance of this ESP may be caused by varying levels of fractionation of Hg species in the flue gas at the **TP**; Hg^0 was the dominant species present, but the ESP removes mainly Hg^{2+} and Hg^p (Wang et al., 2008).

In the coal-fired boiler, the Hg in flue gas exists mainly in the forms of Hg^0 and Hg^2, and the proportion of Hg^p ranged from 0% to 45.13% (Wang et al., 2009). On the other hand, the proportion of Hg^p in the flue

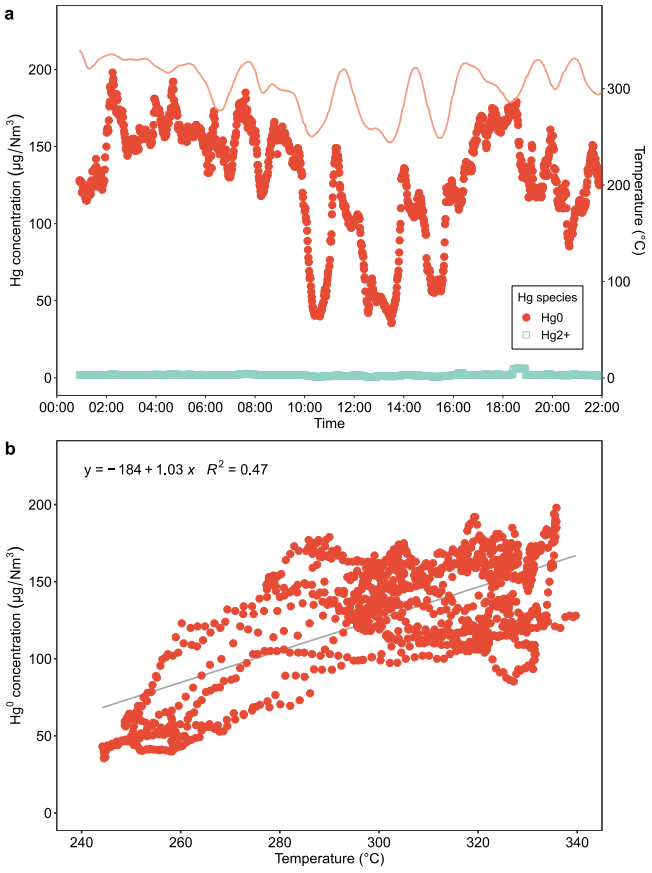

Fig. 3. Relationship between Hg concentrations in flue gas and the temperature at the middle of the furnace: (a) concentrations of Hg^0 and Hg^{2+} in the flue gas from the secondary combustion furnace, and (b) dependence of Hg^0 concentrations on temperatures.

gas was 3.6% before it was treated at the ESP. The lower Hg^p proportion might be related to the absence (or a lower concentration in practice) of the fly ash, as no combustion components in the solid phase were generated according to thermodynamic calculation results. The secondary combustion furnace in this study only incinerated the pyrolysis gas and auxiliary fuels (Table A.2) rather than sewage sludge or coals. Thus, fine particles and unburned carbon, which often occur in fly ash and are reported to enhance the Hg capture, especially the Hg removal at the ESP (Gale et al., 2008; Świerczok et al., 2020), were barely formed. As a result, the concentration of THg emitted from the stack was 98.17 μg/Nm^3, which is higher than the regulatory standard for existing waste treatment plants in Japan of 50 μg/Nm^3. This concentration was also higher than the Hg concentrations monitored in the flue gas of sludge mono-incinerators in our previous research because a large amount of air was utilized during incineration, generating a larger amount of flue gas and diluting the concentration of Hg (Cheng et al., 2020).

3.1.4. Wastewater

The overall Hg concentration in treated water, which was partially recycled to generate steam for the sludge drier, was less than 0.0005 mg/L, which was similar to the level in wastewater from the WSD (Table 1). Thus, the drying process did not change the Hg distribution, as explained above. However, in the wastewater from the WS, THg was elevated to 0.089 mg/L (Table 1). This increase in the Hg concentration in the WS is considered to be associated with Hg speciation (Fig. 2(b)), as Hg^{2+} is absorbed more readily in water, while Hg^0 escapes in the flue gas (Yang et al., 2007). The total suspended solids (*TSS*) in the treated water also had a higher Hg concentration (0.95 mg/kg) than that in the bulk treated water. After treatment in the WS, the Hg concentration was more than 500 fold (520 mg/kg) greater in the *TSS* in wastewater than in treated water. Thus, removal of *TSS* before reuse or discharge of the treated wastewater can efficiently control Hg accumulation within or emission from sewage sludge torrefaction plants. The total wastewater was a mixture of wastewater from the WSD, WS, and ESP. As the ESP removes fine particles (Wang et al., 2010) and is cleaned with water, it increases *TSS* levels while lowering the Hg concentration in *TSS* via dilution.

In conclusion, during sludge torrefaction, the dominant Hg species evolved from Hg^{2+} to Hg^0. Hg^{2+} was dominant in the sludge and remained in the dried sludge. During the torrefaction stage, Hg^{2+} was reduced to Hg^0 under an inert atmosphere of N_2 and was entrained in the pyrolysis gas. Thus, torrefaction was able to separate Hg from the sludge. After the secondary combustion stage, Hg^0 remained the dominant species in the APCDs; Hg^{2+}, on the other hand, was generally removed from the flue gas and discharged into wastewater, especially in the form of *TSS*. As wastewater from the **TP** is recycled in the wastewater treatment process during the earlier sludge treatment stage, Hg bound to *TSS* will be condensed in the sludge again and will continue circulating throughout the whole wastewater and sludge treatment process. Therefore, *TSS* removal from the wastewater prior to discharge can effectively reduce the Hg load release into the environment.

3.2. Hg mass balance in the torrefaction furnace

The hourly flow of Hg in the **TP** is shown in Fig. 1. A total of 1.4 g Hg from the sewage sludge was fed to the furnace. During the drying process, less than 0.03 g/h Hg was discharged into the wastewater. Thus, after drying, no decrease in the Hg concentration occurred in the dried sludge. Instead, the level of Hg was higher in dried sludge (1.5 g/h) than in dewatered sludge (1.4 g/h), which might be due to inhomogeneity of the sludge or discrepancies in sampling and measurement (Tomasi Morgano et al., 2018). In general, the drying process at 100 °C did not affect the behavior of Hg, in accordance with our previous research on sludge drying (110–130 °C) in a step grate stoker (Cheng et al., 2020).

After torrefaction, 0.04 g/h Hg remained in the generated biofuel, which is only 3% of the THg input from the dewatered sludge. A similar result was reported from woody biomass torrefaction at 200–350 °C (Dziok, 2020) and in the sewage sludge pyrolysis process, in which very little Hg was recovered in the char derived from sludge pyrolysis at 350–500 °C under a nitrogen atmosphere (Tomasi Morgano et al., 2018). The low boiling point of Hg favors its early release (US EPA, 2005) and may enable the low recovery of Hg in biofuel (char) (Tomasi Morgano et al., 2018; Yoshida and Antal, 2009).

The remaining Hg was entrained in the flue gas and treated in the APCDs. After treatment in the cyclone, 0.6 g/h Hg was detected at the inlet of the WS, and Hg^0 accounted for 67% of this Hg. Then, from the WS, ESP, and stack, the amount of Hg in the flue gas was nearly constant, and Hg was scarcely removed by these units.

Low Hg removal at the WS was related mainly to the dominant Hg species present, as Hg^0 occurred in the flue gas and was re-emitted at the WS (Cheng et al., 2020). During torrefaction, sulfur (S) in the sludge is partially distributed in the gas phase in the form of H_2S (Liu et al., 2015; Saleh et al., 2014; Tomasi Morgano et al., 2018). H_2S is incinerated and oxidized into SO_x (mainly SO_2 and SO_3) in the secondary combustion furnace and then absorbed into slurry at the WS in the form of sulfite or bisulfite. Thereafter, Hg^{2+} absorbed by the liquid (slurry) at the WS could be reduced to Hg^0 by aqueous S(IV) and re-emitted (Chang, 2003; Chang and Zhao, 2008; Omine et al., 2012). Although a comparable amount of Hg was found at the outlet of WS, 0.5 g/h Hg was also discharged into the wastewater from the WS, and the mass balance increased at the output of the WS. This discrepancy may be caused by re-emission of Hg from wastewater (slurry) at the WS (Díaz-Somoano et al., 2007); on the other hand, the fluctuation in temperature (250–350 °C) in the torrefaction furnace may induce significant

fluctuations in the Hg concentration (35.4–198 μg/Nm^3) and poor balance in Hg mass flow, as described in Section 3.1.3. As the ESP removed negligible Hg at **TP**, the mass balance also increased after the ESP.

Overall, at the **TP**, the total wastewater from the WSD, WS, and ESP contained 57% of the THg, which is slightly less than the amount removed by sewage sludge incinerators (51–83%) in our previous study in Japan (Cheng et al., 2020). In wastewater, 36% of the THg was dissolved in wastewater, and 21% was bound to *TSS*. A slightly higher fraction of Hg (43%) was emitted from the stack of the **TP** than from sludge incinerators (6–33%). However, this difference was not significant. Hg^0 was the dominant species of Hg in the flue gas, accounting for 98% of the total, whereas the Hg^{2+} (1.6%) and Hg^p (0.3%) fractions were almost negligible. The biofuel generated at the **TP** retained only 3% of the Hg in the original sludge.

After the torrefaction process, little Hg remained in the solid phase used as biofuel. In the gas phases of both the torrefaction furnace and secondary combustion furnace, Hg^0 was the dominant species of Hg. At the APCDs, with decreasing temperature, Hg^0 partially evolved into Hg^{2+}, which was then removed from the WS in wastewater. The ESP removed Hg^p but showed poor performance in terms of overall Hg removal. Hg^0 remained the dominant species of Hg emitted from the stack. Thus, the existing APCDs at the **TP**, including a cyclone, WS, and ESP, are insufficient for Hg removal.

3.3. *Adsorptive removal of Hg by a polymer tower in the sewage sludge torrefaction furnace*

Adsorbents are reportedly effective for Hg^0 removal from flue gas. The SPC composite material can adsorb Hg^0 (Abraham et al., 2018; Hasell et al., 2016) due to its structural diversity, tunable pore size, high surface area, chemical stability (Aguila et al., 2017), and resistance to moisture or dust. As Hg^0 is dominant in flue gas from the secondary combustion furnace at **TP**, with the possible presence of moisture and dust, we used GMCS, a type of SPC, to remove Hg from the flue gas.

Fig. 4(a) shows the Hg adsorptive removal performance of the GMCS. At the inlet of the GMCS, the Hg concentration was unstable, which may be due to temperature instability (Section 3.1.3 and Fig. 3). The average THg concentration at the inlet to the polymer tower was 67.5 μg/Nm^3. In the first layer of the polymer, the THg concentration decreased to approximately 30 μg/Nm^3, with further decreases to 23.3 μg/Nm^3 and 11.2 μg/Nm^3 in the second and third layers, respectively. Relative to the Hg concentration at the inlet, the average Hg removal performance after the first, second, and third layers was 55.5%, 65.5%, and 83.3%, respectively. The Hg removal rate of each layer was stable in our spot adsorption test and showed no breakthrough, even for the first layer (Fig. 4(b)). When we plot the Hg removal rate versus the Hg concentration into each layer, which was 5–10%, we found that the Hg removal rate at every single layer is relatively stable, with a median Hg removal rate of 55.2% (Fig. 5). This was the case despite the lowest layer of Hg removal (layer 2) being at a rate of 5–10%. Thus, a theoretically 91% removal rate after 3 layers and 96% after 4 layers can be achieved based on the field study we conducted.

According to the Japanese emission standard (Takiguchi and Tamura, 2018), the Hg concentration in flue gas should be lower than 50 μg/Nm^3 for existing plants and 30 μg/Nm^3 for newly constructed plants. Therefore, although the GMCS we used has eight layers, the first layer removed sufficient Hg to meet the emission standard, resulting in an average Hg concentration of ~30 μg/Nm^3. For newly constructed plants, two layers would be sufficient to decrease the Hg concentration to less than 30 μg/Nm^3. In conclusion, the GMCS with eight layers exhibited both high Hg removal efficiency and a long lifetime in this study, and a GMCS with fewer layers is an alternative that would be effective at lower cost.

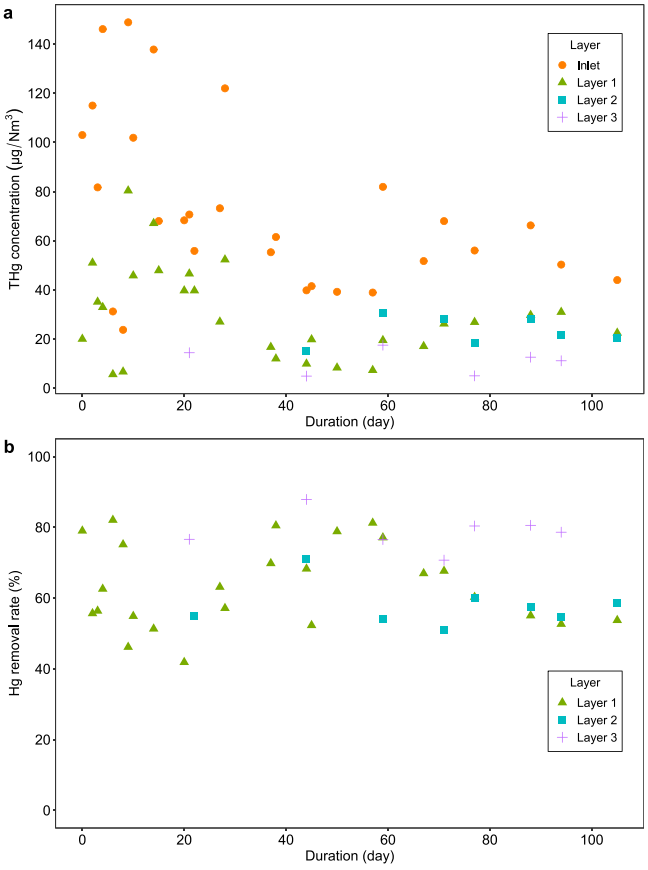

Fig. 4. (a) THg concentration in the inlet and outlet of different layers in the polymer tower at **TP**; (b) Hg removal rate (all based on the inlet THg concentration) after flow through SPC composite material layers 1, 2, and 3.

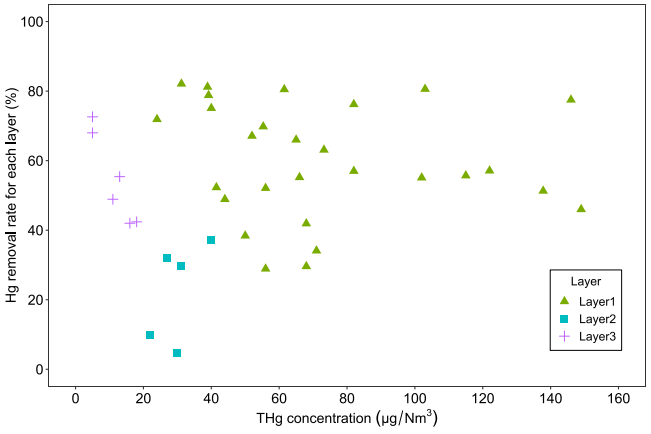

Fig. 5. Hg removal rate for each layer (based on the THg concentration to each layer) in the polymer tower at **TP**.

4. Conclusions

We comprehensively evaluated Hg behavior during sewage sludge torrefaction at a full-scale plant operating in Japan. Our results showed that Hg^0 was the dominant species in both the pyrolysis gas at the torrefaction stage and in the flue gas from the subsequent APCDs. The WS effectively removed Hg^{2+} from the flue gas, and the concentration of Hg bound to *TSS* was much higher than that of dissolved Hg in wastewater from the WS. *TSS* removal from wastewater is therefore recommended for reducing Hg emissions from the wastewater treatment process. The

ESP significantly removed Hg^p but contributed little to overall Hg removal due to the low proportion of Hg^p among Hg species in the flue gas. The existing APCDs at **TP**, which consist of a cyclone, WS, and ESP, are insufficient for Hg removal due to the poor Hg^0 removal performance of the WS and ESP. A commercial SPC composite material, GMCS, was effective in removing Hg after sludge torrefaction. Further research should be conducted on Hg^0 removal from the sludge torrefaction process.

CRediT authorship contribution statement

Yingchao Cheng: Investigation, Writing – original draft, Data curation. **Yuki Asaoka:** Project administration, Investigation. **Yoshiyuki Hachiya:** Project administration, Investigation. **Naoki Moriuchi:** Resources. **Kenji Shiota:** Resources. **Kazuyuki Oshita:** Resources. **Masaki Takaoka:** Conceptualization, Supervision, Writing – review & editing, Funding acquisition.

Supporting information

Additional information about input data to *FactSage* software for torrefaction and secondary combustion furnaces at the **TP**.

Declaration of Competing Interest

The authors declare that they have no known competing financial interests or personal relationships that could have appeared to influence the work reported in this paper.

Acknowledgments

This research was financially supported in part by JSPS KAKENHI grant number JP 17H03335 and the Environment Research and Technology Development Fund of Japan [JPMEERF20S20600]. We thank the local government for managing the sampling process and providing data about the plant.

Appendix A. Supporting information

Supplementary data associated with this article can be found in the online version at doi:10.1016/j.jhazmat.2021.127186.

References

Abraham, A.M., Kumar, S.V., Alhassan, S.M., 2018. Porous sulphur copolymer for gas-phase mercury removal and thermal insulation. Chem. Eng. J. 332, 1–7. https://doi.org/10.1016/j.cej.2017.09.069.

Aguila, B., Sun, Q., Perman, J.A., Earl, L.D., Abney, C.W., Elzein, R., Schlaf, R., Ma, S., 2017. Efficient mercury capture using functionalized porous organic polymer, 1700665 Adv. Mater. 29 (31), 1–6. https://doi.org/10.1002/adma.201700665.

ASTM D6784-02, 2002. D6784-02: standard test method for elemental, oxidized, particle-bound, and total mercury in flue gas generated from coal-fired stationary sources (Ontario-Hydro Method), ASTM International, Pennsylvania, USA.

Atienza-Martínez, M., Fonts, I., ábrego, J., Ceamanos, J., Gea, G., 2013. Sewage sludge torrefaction in a fluidized bed reactor. Chem. Eng. J. 222, 534–545. https://doi.org/10.1016/j.cej.2013.02.075.

Atienza-Martínez, M., Mastral, J.F., Ábrego, J., Ceamanos, J., Gea, G., 2015. Sewage sludge torrefaction in an auger reactor. Energy Fuels 29, 160–170. https://doi.org/10.1021/ef501425h.

Axelsson, L., Franzén, M., Ostwald, M., Berndes, G., Lakshmi, G., Ravindranath, N.H., 2012. Perspective: Jatropha cultivation in southern India: assessing farmers' experiences. Biofuels, Bioprod. Bioref. 6, 246–256. https://doi.org/10.1002/bbb.

Basu, P., 2013. Torrefaction, Biomass Gasification, Pyrolysis and Torrefaction. Elsevier Inc. https://doi.org/10.1016/b978-0-12-396488-5.00004-6.

Cao, Y., Pawłowski, A., 2012. Sewage sludge-to-energy approaches based on anaerobic digestion and pyrolysis: brief overview and energy efficiency assessment. Renew. Sustain. Energy Rev. 16, 1657–1665. https://doi.org/10.1016/j.rser.2011.12.014.

Chalkidis, A., Jampaiah, D., Hartley, P.G., Sabri, Y.M., Bhargava, S.K., 2020. Mercury in natural gas streams: a review of materials and processes for abatement and remediation. J. Hazard. Mater. 382, 121036 https://doi.org/10.1016/j.jhazmat.2019.121036.

Chang, J.C., Ghorishi, S.B., 2003. Simulation and evaluation of elemental mercury concentration increase in flue gas across a wet scrubber. Environ. Sci. Technol. 37, 5763–5766. https://doi.org/10.1021/es034352s.

Chang, J.C., Zhao, Y., 2008. Pilot plant testing of elemental mercury reemission from a wet scrubber. Energy Fuels 22, 338–342. https://doi.org/10.1021/ef700355q.

Cheng, C.M., Cao, Y., Kai, Z., Pan, W.P., 2013. Co-effects of sulfur dioxide load and oxidation air on mercury re-emission in forced-oxidation limestone flue gas desulfurization wet scrubber. Fuel 106, 505–511. https://doi.org/10.1016/j.fuel.2012.11.068.

Cheng, L., Wang, L., Geng, Y., Wang, N., Mao, Y., Cai, Y., 2019. Occurrence, speciation and fate of mercury in the sewage sludge of China. Ecotoxicol. Environ. Saf. 186, 109787 https://doi.org/10.1016/j.ecoenv.2019.109787.

Cheng, Y., Oleszek, S., Shiota, K., Oshita, K., Takaoka, M., 2020. Comparison of sewage sludge mono-incinerators: mass balance and distribution of heavy metals in step grate and fluidized bed incinerators. Waste Manag. 105, 575–585. https://doi.org/10.1016/j.wasman.2020.02.044.

Dziok, T., Kołodziejska, E.K., Kołodziejska, E.L., 2020. Mercury content in woody biomass and its removal in the torrefaction process. Biomass Bioenergy 143, 105832. https://doi.org/10.1016/j.biombioe.2020.105832.

Díaz-Somoano, M., Unterberger, S., Hein, K.R., 2007. Mercury emission control in coal-fired plants: the role of wet scrubbers. Fuel Process. Technol. 88, 259–263. https://doi.org/10.1016/j.fuproc.2006.10.003.

Ebert, J., 2013. Innovative new air pollution control technologies to capture NOx, PM and Hg. In: 2013 21st Annual North American Waste-to-Energy Conference, American Society of Mechanical Engineers Digital Collection. ⟨https://doi.org/10.1115/NAWTEC21–2715⟩.

Edwards, J.R., Srivastava, R.K., Kilgroe, J.D., 2001. A study of gas-phase mercury speciation using detailed chemical kinetics. J. Air Waste Manag. Assoc. 51, 869–877. https://doi.org/10.1080/10473289.2001.10464316.

Friedli, H.R., Radke, L.F., Prescott, R., Li, P., Woo, J.H., Carmichael, G.R., 2004. Mercury in the atmosphere around Japan, Korea, and China as observed during the 2001 ACE-Asia field campaign: measurements, distributions, sources, and implications. J. Geophys. Res. Atmos. 109, 1–13. https://doi.org/10.1029/2003JD004244.

Galbreath, K.C., Zygarlicke, C.J., 2000. Mercury transformations in coal combustion flue gas. Fuel Process. Technol. 65, 289–310. https://doi.org/10.1016/S0378-3820(99)00102-2.

Gale, T.K., Lani, B.W., Offen, G.R., 2008. Mechanisms governing the fate of mercury in coal-fired power systems. Fuel Process. Technol. 89, 139–151. https://doi.org/10.1016/j.fuproc.2007.08.004.

Hasell, T., Parker, D.J., Jones, H.A., Mcallister, T., Howdle, S.M., 2016. Porous inverse vulcanised polymers for mercury capture. Chem. Commun. 52, 5383–5386. https://doi.org/10.1039/C6CC00938G.

Holmes, P., James, K.A.F., Levy, L.S., 2009. Is low-level environmental mercury exposure of concern to human health? Sci. Total Environ. 408, 171–182. https://doi.org/10.1016/j.scitotenv.2009.09.043.

Hsu, C.J., Atkinson, J.D., Chung, A., Hsi, H.C., 2021. Gaseous mercury re-emission from wet flue gas desulfurization wastewater aeration basins: a review. J. Hazard. Mater., 126546 https://doi.org/10.1016/j.jhazmat.2021.126546.

Janowska, B., Szymański, K., Sidełko, R., Siebielska, I., Walendzik, B., 2017. Assessment of mobility and bioavailability of mercury compounds in sewage sludge and composts. Environ. Res. 156, 394–403. https://doi.org/10.1016/j.envres.2017.04.005.

Kellie, S., Cao, Y., Duan, Y., Li, L., Chu, P., Mehta, A., Carty, R., Riley, J.T., Pan, W.P., 2005. Factors affecting mercury speciation in a 100-MW coal-fired boiler with low-NOx burners. Energy Fuels 19, 800–806. https://doi.org/10.1021/ef049769d.

Lei, C., Yufeng, D., Yuqun, Z., Liguo, Y., Liang, Z., Xianghua, Y., Qiang, Y., Yiman, J., Xuchang, X., 2007. Mercury transformation across particulate control devices in six power plants of China: the co-effect of chlorine and ash composition. Fuel 86, 603–610. https://doi.org/10.1016/j.fuel.2006.07.030.

Li, H., Feng, K., 2018. Life cycle assessment of the environmental impacts and energy efficiency of an integration of sludge anaerobic digestion and pyrolysis. J. Clean. Prod. 195, 476–485. https://doi.org/10.1016/j.jclepro.2018.05.259.

Liu, M., Du, P., Yu, C., He, Y., Zhang, H., Sun, X., Lin, H., Luo, Y., Xie, H., Guo, J., Tong, Y., Zhang, Q., Chen, L., Zhang, W., Li, X., Wang, X., 2018. Increases of total mercury and methylmercury releases from municipal sewage into environment in China and implications. Environ. Sci. Technol. 52, 124–134. https://doi.org/10.1021/acs.est.7b05217.

Liu, S., Wei, M., Qiao, Y., Yang, Z., Gui, B., Yu, Y., Xu, M., 2015. Release of organic sulfur as sulfur-containing gases during low temperature pyrolysis of sewage sludge. Proc. Combust. Inst. 35, 2767–2775. https://doi.org/10.1016/j.proci.2014.06.055.

Löthgren, C.J., Takaoka, M., Andersson, S., Allard, B., Korell, J., 2007. Mercury speciation in flue gases after an oxidative acid wet scrubber. Chem. Eng. Technol. 30, 131–138. https://doi.org/10.1002/ceat.200600172.

Mayer, B.K., Baker, L.A., Boyer, T.H., Drechsel, P., Gifford, M., Hanjra, M.A., Parameswaran, P., Stoltzfus, J., Westerhoff, P., Rittmann, B.E., 2016. Total value of phosphorus recovery. Environ. Sci. Technol. 50, 6606–6620. https://doi.org/10.1021/acs.est.6b01239.

Meij, R., te Winkel, H., 2006. Mercury emissions from coal-fired power stations: the current state of the art in the Netherlands. Sci. Total Environ. 368, 393–396. https://doi.org/10.1016/j.scitotenv.2005.09.083.

MLIT (Ministry of Land, Infrastructure, Transport and Tourism), List of commercial sweage sludge torrefaction or cabonization plants ⟨https://www.mlit.go.jp/mizukokudo/sewerage/content/001366941.pdf⟩(Accessed 30 May 2021).

Mulchandani, A., Westerhoff, P., 2016. Recovery opportunities for metals and energy from sewage sludges. Bioresour. Technol. 215, 215–226. https://doi.org/10.1016/j.biortech.2016.03.075.

Omine, N., Romero, C.E., Kikkawa, H., Wu, S., Eswaran, S., 2012. Study of elemental mercury re-emission in a simulated wet scrubber. Fuel 91, 93–101. https://doi.org/10.1016/j.fuel.2011.06.018.

Pacyna, E.G., Pacyna, J.M., Sundseth, K., Munthe, J., Kindbom, K., Wilson, S., Steenhuisen, F., Maxson, P., 2010. Global emission of mercury to the atmosphere from anthropogenic sources in 2005 and projections to 2020. Atmos. Environ. 44, 2487–2499. https://doi.org/10.1016/j.atmosenv.2009.06.009.

Park, S.W., Jang, C.H., 2011a. Characteristics of carbonized sludge for co-combustion in pulverized coal power plants. Waste Manag. 31, 523–529. https://doi.org/10.1016/j.wasman.2010.10.009.

Park, S.W., Jang, C.H., 2011b. Effects of carbonization and solvent-extraction on change in fuel characteristics of sewage sludge. Bioresour. Technol. 102, 8205–8210. https://doi.org/10.1016/j.biortech.2011.05.072.

Peccia, J., Westerhoff, P., 2015. We should expect more out of our sewage sludge. Environ. Sci. Technol. 49, 8271–8276. https://doi.org/10.1021/acs.est.5b01931.

Preciado, I., Young, T., Silcox, G., 2014. Mercury oxidation by halogens under air- and oxygen-fired conditions. Energy Fuels 28, 1255–1261. https://doi.org/10.1021/ef402074p.

Prins, M.J., Ptasinski, K.J., Janssen, F.J.J.G., 2006. Torrefaction of wood: part 2. Analysis of products. J. Anal. Appl. Pyrolysis 77, 35–40. https://doi.org/10.1016/j.jaap.2006.01.001.

Raheem, A., Sikarwar, V.S., He, J., Dastyar, W., Dionysiou, D.D., Wang, W., Zhao, M., 2018. Opportunities and challenges in sustainable treatment and resource reuse of sewage sludge: a review. Chem. Eng. J. 337, 616–641. https://doi.org/10.1016/j.cej.2017.12.149.

Reed, G.P., Ergüdenler, A., Grace, J.R., Watkinson, A.P., Herod, A.A., Dugwell, D., Kandiyoti, R., 2001. Control of gasifier mercury emissions in a hot gas filter: the effect of temperature. Fuel 80, 623–634. https://doi.org/10.1016/S0016-2361(00)00148-4.

Saleh, S.B., Flensborg, J.P., Shoulaifar, T.K., Sa, Z., Hansen, B.B., Egsgaard, H., Demartini, N., Jensen, P.A., Glarborg, P., Dam-johansen, K., 2014. Release of chlorine and sulfur during biomass torrefaction and pyrolysis. Energy Fuels 28, 3738–3746. https://doi.org/10.1021/ef4021262.

Santos, A., Judd, S., 2010. The fate of metals in wastewater treated by the activated sludge process and membrane bioreactors: a brief review. J. Environ. Monit. 12, 110–118. https://doi.org/10.1039/b918161j.

Sloss, L.L., 2017. Emerging markets for pollution control retrofits. ⟨https://usea.org/publication/emerging-markets-pollution-control-retrofits-ccc-274⟩.

Song, Y.C., Kwon, S.J., Woo, J.H., 2004. Mesophilic and thermophilic temperature co-phase anaerobic digestion compared with single-stage mesophilic- and thermophilic digestion of sewage sludge. Water Res. 38, 1653–1662. https://doi.org/10.1016/j.watres.2003.12.019.

Srivastava, R.K., Hutson, N., Martin, B., Princiotta, F., Staudt, J., 2006. Control of mercury emissions from coal-fired electric utility boilers. Environ. Sci. Technol. 40, 1385–1393. https://doi.org/10.1021/es062639u.

Stasinakis, A.S., 2012. Review on the fate of emerging contaminants during sludge anaerobic digestion. Bioresour. Technol. 121, 432–440. https://doi.org/10.1016/j.biortech.2012.06.074.

Świerczok, A., Jędrusik, M., Łuszkiewicz, D., 2020. Reduction of mercury emissions from combustion processes using electrostatic precipitators. J. Electrostat. 104. https://doi.org/10.1016/j.elstat.2020.103421.

Takahashi, F., Kida, A., Shimaoka, T., 2010. Statistical estimate of mercury removal efficiencies for air pollution control devices of municipal solid waste incinerators. Sci. Total Environ. 408, 5472–5477. https://doi.org/10.1016/j.scitotenv.2010.07.067.

Takaoka, M., Domoto, S., Oshita, K., Takeda, N., Morisawa, S., 2012. Mercury emission from sewage sludge incineration in Japan. J. Mater. Cycles Waste Manag. 14, 113–119. https://doi.org/10.1007/s10163-012-0044-2.

Takaoka, M., Oshita, K., Okada, M., Watanabe, T., Tanida, K., 2018. Mercury behaviour in flue gas from sewage sludge incinerators and melting furnace. Water Sci. Technol. 2017, 782–790. https://doi.org/10.2166/wst.2018.268.

Takaoka, M., Takeda, N., Fujiwara, T., Kurata, M., Kimura, T., 2002. Control of mercury emissions from a municipal solid waste incinerator in Japan. J. Air Waste Manag. Assoc. 52, 931–940. https://doi.org/10.1080/10473289.2002.10470831.

Takiguchi, H., Tamura, T., 2018. Mercury emission control in Japan. Asian J. Atmos. Environ. 12, 37–46. https://doi.org/10.5572/ajae.2018.12.1.037.

Tasca, A.L., Puccini, M., Gori, R., Corsi, I., Galletti, A.M.R., Vitolo, S., 2019. Hydrothermal carbonization of sewage sludge: a critical analysis of process severity, hydrochar properties and environmental implications. Waste Manag. 93, 1–13. https://doi.org/10.1016/j.wasman.2019.05.027.

Titirici, M.M., Thomas, A., Antonietti, M., 2007. Back in the black: hydrothermal carbonization of plant material as an efficient chemical process to treat the CO_2 problem? N. J. Chem. 31, 787–789. https://doi.org/10.1039/b616045j.

Tomasi Morgano, M., Leibold, H., Richter, F., Stapf, D., Seifert, H., 2018. Screw pyrolysis technology for sewage sludge treatment. Waste Manag. 73, 487–495. https://doi.org/10.1016/j.wasman.2017.05.049.

Tumuluru, J.S., Sokhansanj, S., Hess, J.R., Wright, C.T., Boardman, R.D., 2011. A review on biomass torrefaction process and product properties for energy applications. Ind. Biotechnol. 7, 384–401. https://doi.org/10.1089/ind.2011.7.384.

US EPA, 2001. Mercury in petroleum and natural gas: estimation of emissions from production, processing and combustion, Research Triangle Park, NC, United States.

US EPA, 2005. Control of mercury emissions from coal fired electric utility boilers: an update, 59.

Van Wesenbeeck, S., Prins, W., Ronsse, F., Antal, M.J., 2014. Sewage sludge carbonization for biochar applications. Fate of heavy metals. Energy Fuels 28, 5318–5326. https://doi.org/10.1021/ef500875c.

Wang, S.X., Zhang, L., Li, G.H., Wu, Y., Hao, J.M., Pirrone, N., Sprovieri, F., Ancora, M.P., 2010. Mercury emission and speciation of coal-fired power plants in China. Atmos. Chem. Phys. 10, 1183–1192. https://doi.org/10.5194/acp-10-1183-2010.

Wang, Y., Duan, Y., Yang, L., Jiang, Y., Wu, C., Wang, Q., Yang, X., 2008. Comparison of mercury removal characteristic between fabric filter and electrostatic precipitators of coal-fired power plants. J. Fuel Chem. Technol. 36, 23–29. https://doi.org/10.1016/s1872-5813(08)60009-2.

Wang, Y., Duan, Y., Yang, L., Zhao, C., Shen, X., Zhang, M., Zhuo, Y., Chen, C., 2009. Experimental study on mercury transformation and removal in coal-fired boiler flue gases. Fuel Process. Technol. 90, 643–651. https://doi.org/10.1016/j.fuproc.2008.10.013.

Westerhoff, P., Lee, S., Yang, Y., Gordon, G.W., Hristovski, K., Halden, R.U., Herckes, P., 2015. Characterization, recovery opportunities, and valuation of metals in municipal sludges from US wastewater treatment plants nationwide. Environ. Sci. Technol. 49, 9479–9488. https://doi.org/10.1021/es505329q.

Xu, Z.X., Song, H., Li, P.J., He, Z.X., Wang, Q., Wang, K., Duan, P.G., 2020. Hydrothermal carbonization of sewage sludge: Effect of aqueous phase recycling. Chem. Eng. J. 387. https://doi.org/10.1016/j.cej.2019.123410.

Yang, H., Xu, Z., Fan, M., Bland, A.E., Judkins, R.R., 2007. Adsorbents for capturing mercury in coal-fired boiler flue gas. J. Hazard. Mater. 146, 1–11. https://doi.org/10.1016/j.jhazmat.2007.04.113.

Yoshida, T., Antal, M.J., 2009. Sewage sludge carbonization for terra preta applications. Energy Fuels 23, 5454–5459. https://doi.org/10.1021/ef900610k.

Zhang, L., Wang, S., Meng, Y., Hao, J., 2012. Influence of mercury and chlorine content of coal on mercury emissions from coal-fired power plants in China. Environ. Sci. Technol. 46, 6385–6392. https://doi.org/10.1021/es300286n.

Zhang, L., Wong, M.H., 2007. Environmental mercury contamination in China: sources and impacts. Environ. Int. 33, 108–121. https://doi.org/10.1016/j.envint.2006.06.022.

Zhang, Q., Hu, J., Lee, D.J., Chang, Y., Lee, Y.J., 2017. Sludge treatment: current research trends. Bioresour. Technol. 243, 1159–1172. https://doi.org/10.1016/j.biortech.2017.07.070.

Zhao, Y., Ren, Q., Na, Y., 2018. Phosphorus transformation from municipal sewage sludge incineration with biomass: formation of apatite phosphorus with high bioavailability. Energy Fuels 32, 10951–10955. https://doi.org/10.1021/acs.energyfuels.8b01915.

Zheng, C., Ma, X., Yao, Z., Chen, X., 2019. The properties and combustion behaviors of hydrochars derived from co-hydrothermal carbonization of sewage sludge and food waste. Bioresour. Technol. 285, 121347 https://doi.org/10.1016/j.biortech.2019.121347.